^{29}Si and ^{13}C NMR Investigation of the Polysilane-to-Poly(carbosilane) Conversion of Poly(methylchlorosilanes) Using Cross-Polarization and Inversion Recovery Cross-Polarization Techniques

Florence Babonneau,* Jocelyne Maquet, and Christian Bonhomme

Chimie de la Matière Condensée, Université Pierre et Marie Curie/CNRS, 4 place Jussieu, 75005 Paris, France

Robin Richter and Gerhard Roewer

Department of Inorganic Chemistry, Freiberg University of Mining and Technology, D-09596 Freiberg, Germany

Djamila Bahloul

Laboratoire des Céramiques Nouvelles, Faculté des Sciences de Limoges, 123 Avenue A. Thomas, 87060 Limoges, France

Received January 2, 1996. Revised Manuscript Received May 1, 1996[⊗]

The polysilane-to-polycarbosilane transformation of polymethylchlorosilane prepared from based-catalyzed disproportionation of 1,1,2,2-tetrachlorodimethyldisilane has been characterized in detail by ^{29}Si and ^{13}C magic angle spinning nuclear magnetic resonance, using cross-polarization as well as inversion recovery cross-polarization techniques. These techniques allow a clear insight in the protonated environment of a given nucleus, in particular to distinguish between strongly coupled nuclei such as $^{13}CH_2$ and moderately coupled ones such as $^{13}CH_3$. For the first time, the IRCP sequence was also used to probe the environment of ^{29}Si nuclei in such systems and proved to be very effective in distinguishing the silane and carbosilane sites. The 180−450 °C temperature range was investigated: the formation of carbosilane units was clearly demonstrated by ^{13}C and also ^{29}Si NMR experiments. The various ^{29}Si and ^{13}C sites were thus identified due to their polarization inversion behavior and quantified. Comparison of these results with a thermogravimetric analysis coupled with mass spectrometry allowed us to propose two different mechanisms for the formation of carbosilane units in such system: at low temperature ($T \geq 180$ °C), it is suggested that carbosilane units are formed via condensation reactions between Si−Cl and H−C groups, while at higher temperature ($T \geq 380$ °C), the so-called "Kumada rearrangement" occurs.

I. Introduction

Chemical routes using molecular or polymeric precursors offer significant potential for the fabrication of novel ceramic shapes at very low processing temperatures relative to those required in typical melt or solid-state ceramic processing approaches. The most studied one is the sol−gel process which has been employed to obtain oxide glasses and ceramics.[1] The network is formed from hydrolysis−condensation reactions of precursors such as mineral salts or metallic alkoxides. A polymer route has also been developed for the preparation of non-oxide ceramics such as carbides and nitrides.[2−5] Its feasibility was first demonstrated by Yajima[6] in 1975 and led to the commercialization of Nicalon silicon carbide fibers.[7]

One main advantage of such approaches is the possibility to tailor monomers and polymers in order to dictate the nano- and/or microstructure as well as the phases desired in the target ceramic product. Currently, it is still rather difficult to predict what types of polymer architecture will lead to selected ceramic products under specific pyrolysis conditions. One reason is a lack of deep understanding of the chemical reactions that occur during the cross-linking and pyrolysis processes. Most of the intermediates are insoluble, predominantly amorphous, and their structural characterization is thus rather difficult. Nuclear magnetic resonance (NMR) using magic angle spinning (MAS) has emerged as a powerful, nondestructive tool to characterize such materials. Indeed, the large range of ^{29}Si resonances allows an identification of the Si sites: the numerous studies performed on various types of polysilanes and polycarbosilanes have lead to a scale for the chemical shift of sites such as $SiC_{4-x}H_x$, $SiC_{4-x}Si_x$, and even $SiC_{4-x}O_x$ and $SiC_{4-x}N_x$ in the case of poly(carbosiloxanes) and polysilazanes, respectively.[8] This has been

[⊗] Abstract published in *Advance ACS Abstracts,* June 15, 1996.

(1) Brinker C. J.; Scherrer, G. W. *Sol-Gel Science*; Academic Press: New York, 1990.
(2) Wynne, K. J.; Rice, R. W. *Annu. Rev. Mater. Sci.* **1984**, *14*, 297.
(3) Pouskouleli, G. *Ceram. Int.* **1989**, *15*, 213.
(4) Peuckert, M.; Vaahs, T.; Brück, M. **1990**, *2*, 398.
(5) Laine, R. M.; Babonneau, F. *Chem. Mater.* **1993**, *5*, 260.
(6) Yajima, S.; Hayashi, J.; Omori, M. *Chem. Lett.* **1975**, 931.
(7) Yajima, S. In *Handbook of Composites*; Watt, W., Perov, B. V., Eds.; Elsevier Science Publishers: Dordrecht, 1985; Vol. 1, p 201.

S0897-4756(96)00002-6 CCC: $12.00

extensively used to follow the pyrolysis process of these polymers. Identification of the C sites is more difficult due to the large overlap of the resonance signals which is usually observed. The best example is the well known Yajima polymer which presents a ^{13}C MAS NMR spectrum with a broad signal in which it is impossible to identify directly CH_3 and CH_2 groups.[9] Identification of the various CH_x sites is even more difficult on pyrolyzed samples when the signals broaden due to chemical shift distribution and are strongly overlapped. Usually a downfield shift is observed that indicates that deprotonation reactions occur with the transformation of CH_3 groups into CH_2, CH, and finally into quaternary $C(Si)_4$ sites.[10] However, no reliable quantification can be carried out.

In solution NMR, several spectral editing techniques such as DEPT and INEPT[11] have been used to differentiate signals based on the number of directly bonded protons. These techniques take advantage of the *J* couplings, for example, $^{13}C-^{1}H$. In the solid state, similar spectral editing methods have been developed. They are based on cross-polarization (CP) sequences and thus use $^{13}C-^{1}H$ dipolar couplings. They are usually combined with magic angle spinning (MAS) and high-power proton decoupling. One of the most used is the delayed decoupling sequence NQS (nonquaternary suppression), based on dipolar dephasing[12,13] which is quite effective in differentiating between strongly coupled sites (i.e., rigid ^{13}CH and $^{13}CH_2$) and moderately or weakly coupled sites (i.e., quaternary ^{13}C and $^{13}CH_3$). Unfortunately, it is now well-known that the distinction between strongly coupled ^{13}C sites such as ^{13}CH and $^{13}CH_2$ is not straightforward. More recently, a new sequence, based on inversion of polarization (inversion recovery cross polarization, IRCP) has been proposed in order to get a complete spectral editing in CP MAS NMR.[14−18] The principle of this sequence is presented in Figure 1. The only modification compared to the classical CP sequence is the introduction of a phase inversion during the contact time. The first step consists in polarizing all of the CH_n groups during a relatively long contact time, t_c. After the phase inversion, the spin polarization will progressively invert during an inversion time, t_i. The dynamics of inversion is similar to the polarization dynamics in a standard CP sequence,[19] and thus strongly depends on the $^{13}C-^{1}H$ dipolar coupling: this sequence is therefore very sensitive to the local proton environment and molecular motion. A careful analysis of the CP dynamics allows a clear distinction between the various $^{13}CH_x$ sites depending on the *x* value and also between rigid and

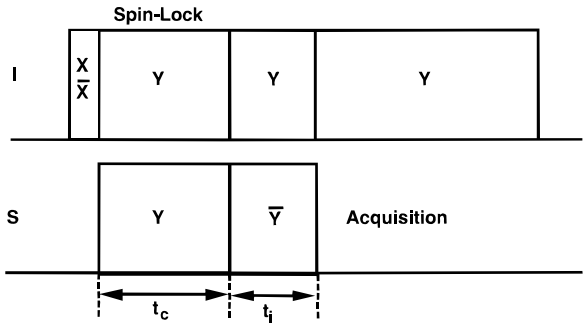

Figure 1. IRCP pulse sequence.

mobile $^{13}CH_x$ sites. The main advantage of this sequence compared to the standard CP sequence is that the magnetization starts from an optimum value, then decreases and becomes negative when increasing t_i. It is thus easy to visualize differences in inversion dynamics of various signals especially when they overlap. On the basis of theoretical arguments, the relative rates of polarization are expected to be as follows:[20]

$$CH_3(\text{static}) > CH_2 > CH \approx CH_3(\text{rotating}) \gg C(\text{nonprotonated})$$

This was illustrated theoretically and experimentally in organic[16−18,21,22] and organometallic compounds,[23] polymers, and coals.[15−18] This technique has been applied to very few nuclei besides ^{13}C: one paper presents a study of amorphous hydrogenated silicon using ^{29}Si IRCP MAS NMR.[24] More recently, IRCP sequence has been successfully applied to study the CP dynamics of various $^{15}NH_x$ sites in simple organic molecules.[25]

Such a technique appears very attractive for following the various steps of the polymer-to-ceramic transformation in a large variety of preceramic polymers—polysilanes, polycarbosilanes, polysilazanes, polyborazines—for which the C and/or N environments are strongly modified during pyrolysis. In the present paper, IRCP coupled with CP experiments have been used to characterize the polysilane−poly(carbosilane) transformation of methylchloropolysilanes (MCPS) which occurs in the 200−450 °C temperature range. MCPS can be prepared in one step by a Lewis-base-catalyzed disproportionation of methylchlorodisilanes. These disilanes are byproducts of the synthesis of methylchlorosilanes (Müller−Rochow process).[26] For the present study, 1,1,2,2-tetrachlorodimethyldisilane, ($MeCl_2Si-SiCl_2Me$, **2**) was disproportionated under heterogeneous conditions, which allows one to separate the formed oligomers free from the catalyst using catalytically active dimethylamidophosphoryl groups (D) grafted onto a silicate carrier (eq 1). The methylchlorooligosilanes **3**−**7** that are formed at 175 °C were fully characterized by liquid-phase NMR spectroscopy up to the heptasilane **7**.[26,27]

(8) Gérardin, C.; Henry, M.; Taulelle, F. In *Better Ceramics through Chemistry V*; Hampden-Smith, M. J., Klemperer, W. G., Brinker, C. J., Eds.; Mat. Res. Soc. Symp. Proc. Vol. 271, 1992; p 777.
(9) Sorarù, G. D.; Babonneau, F.; Mackenzie, J. D. *J. Mater. Sci.* **1990**, *25*, 3886.
(10) Schmidt, W. R.; Interrante, L. V.; Doremus, R. H.; Trout, T. K.; Marchetti, P. S.; Maciel, G. E. *Chem. Mater.* **1991**, *3*, 257.
(11) Derome, A. E. *Modern NMR Techniques for Chemistry Research*; Pergamon Press: New York, 1987.
(12) Alla, M.; Lippmaa, E. *Chem. Phys. Lett.* **1976**, *37*, 260.
(13) Opella, S. J.; Frey, M. H. *J. Am. Chem. Soc.* **1979**, *101*, 5854.
(14) Cory, D. G.; Ritchey, W. M. *Macromolecules* **1989**, *22*, 1611.
(15) Tekely, P.; Montigny, F.; Canet, D.; Delpuech, J. J. *Chem. Phys. Lett.* **1990**, *175*, 401.
(16) Wu, X.; Zilm, K. W. *J. Magn. Reson.* **1993**, *A102*, 205.
(17) Palmas, P.; Tekely, P.; Canet, D. *J. Magn. Reson.* **1993**, *A104*, 26.
(18) Sangill, R.; Rastrup-Andersen, N.; Bildsoe, H.; Jakobsen, H. J.; Nielsen, N. C. *J. Magn. Reson.* **1994**, *A107*, 67.
(19) Wu, X.; Zhang, S. *Chem. Phys. Lett.* **1989**, *156*, 79.
(20) Alemany, L. B.; Grant, D. M.; Pugmire, R. J.; Alger, T. D.; Zilm, K. W. *J. Am. Chem. Soc.* **1983**, *105*, 2142.
(21) Hirschinger, J.; Hervé, M. *Solid State Magn. Reson.* **1994**, *3*, 121.
(22) Wu, X.; Burns, S. T.; Zilm, K. W. *J. Magn. Reson.* **1994**, *A111*, 29.
(23) Bonhomme, C.; Maquet, J.; Livage, J.; Mariotto, G. *Inorg. Chim. Acta* **1995**, *230*, 85.
(24) Zumbulyadis, N. *J. Chem. Phys.* **1987**, *86*, 1162.
(25) Bonhomme, C.; Babonneau, F.; Maquet, J.; Livage, J.; Vaultier, M.; Framery, E. *J. Chim. Phys.* **1995**, *92*, 1881.
(26) Herzog, U.; Richter, R.; Brendler, E.; Roewer, G. *J. Organomet. Chem.* **1996**, *507*, 221.

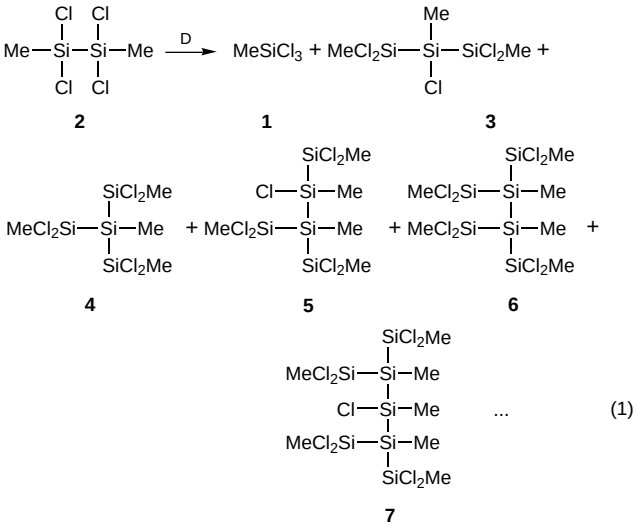

For higher reaction temperatures, cross-linking of the oligosilanes occurs. The solid samples investigated in the present study have been obtained for reaction temperatures ranging from 180 to 450 °C. The main objective was to follow the polysilane-to-polycarbosilane conversion and to clearly identify the formation of Si−CH_2−Si groups, by combining ^{13}C and ^{29}Si CP and IRCP MAS NMR experiments.

II. Experimental Section

II.1. Synthesis of the Polymers. MCPS was prepared by Lewis-base-catalyzed disproportionation of 1,1,2,2-tetrachlorodimethyldisilane ($MeCl_2Si-SiCl_2Me$) under heterogeneous conditions. The disilane fraction of the Müller−Rochow synthesis was treated with $AlCl_3$ and MeCOCl to obtain the pure disilane.[28] A silicate carrier superficially modified with bis(dimethylamido)phosphoryl groups was applied as catalyst.[29] The synthetic procedure has been already described in detail elsewhere.[26,30,31] The polymer samples that have been investigated were cross-linked by heat treatment under a dry argon flow, at various temperatures ranging from 180 to 450 °C with a constant treatment time of 2 h. The as-prepared polymers are not pyrophoric but are obviously oxygen and moisture sensitive.

II.2. NMR Experiments. The spectra were recorded on a Bruker MSL300 spectrometer at 75.47 MHz for ^{13}C and at 59.63 MHz for ^{29}Si with a Bruker CPMAS probe using 7 mm ZrO_2 rotors. All the rotors were filled in a glovebox under a dry argon atmosphere, due to the high air and moisture sensitivity of the samples. The spinning rate was 5 kHz. All the experiments, CP and IRCP, were performed under the same Hartmann−Hahn match condition. Both RF channel levels, $\omega_{1I}/2\pi$ and $\omega_{1S}/2\pi$, were set at about 42 kHz. The ^{13}C NMR spectra were recorded with a spectral width of 30 kHz, using 3K data points in the time domain. The number of transients per spectra varied from 184 to 600, depending on the sample. For each sample, ^{13}C CP MAS NMR spectra were recorded with 12 different contact times, t_c from 10 μs to 30 ms. For the IRCP experiments, a contact time of 3 ms was chosen in order to maximize the polarization of the ^{13}C nuclei. Sixteen spectra were recorded for various inversion times, t_i, from 5 μs to 1 ms. The recycle delays between pulses was 10 s. The ^{29}Si CP MAS NMR spectra were recorded with a spectral width of 24 kHz, using 4K data points with 14 different contact times, from 100 μs to 50 ms. The ^{29}Si IRCP MAS NMR spectra were recorded with a contact time of 5 ms, and with 21 inversion times varying from 5 μs to 4 ms. The recycle delays between pulses was 10 s. Proton decoupling was always applied during acquisition. A 50 Hz line broadening was applied to the FIDs before Fourier transform. The spectra were simulated with the WIN-FIT program.[32]

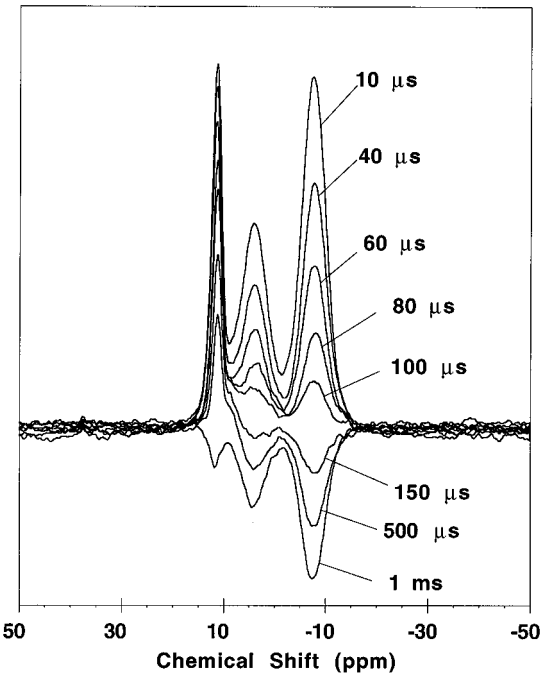

Figure 2. ^{13}C IRCP MAS NMR spectra of the 180 °C MCPS (contact time 3 ms; inversion times are indicated for each spectra).

II.3. TG/MS Experiments. The thermal decomposition was investigated by using a thermogravimetric analyzer (TGA, Netzsch STA 409) interfaced with a quadrupole mass spectrometer (MS, Quadrex 200, Leybold Heraeus, 70 eV, electron impact). The sample was placed in an alumina crucible and weighed in a glovebox. The sample was then heated at 10 °C/min in flowing helium (He N60).

III. Results

III.1. NMR Study of the 180 °C MCPS. The NMR study performed on the MCPS 180 °C will first be presented in detail. Emphasis will be placed on the method used to identify and quantify the various ^{29}Si and ^{13}C sites, through the combination of CP and IRCP techniques.

^{13}C NMR Investigation. The series of ^{13}C IRCP-MAS NMR spectra recorded on the MCPS 180 °C is presented in Figure 2. Three signals are present at around −7, 4, and 11 ppm. The dynamics of inversion of the various peaks is obviously different: the peak at 11 ppm inverts at a higher inversion time, t_i (500 μs < t_i < 1 ms) than the peaks at −7 and 4 ppm (100 μs < t_i < 150 μs). All the spectra have been simulated with the same peaks: chemical shift, line width, and shape were kept constant, only the amplitudes were fitted. The IRCP spectra were first simulated; the number of peaks can be identified by a close observation of the spectra, especially those presenting positive and negative peaks. Once a set of peaks was found to successfully simulate

(27) Brendler, E.; Leo, K.; Thomas, B.; Richter, R.; Roewer, G.; Krämer, H. In *Organosilicon Chemistry II*; Auner, N., Weis, J., Eds.; VCH: Weinheim, 1996; p 69.
(28) Watanabe, H.; Kobayashi, M.; Koike, Y.; Nagashima, S.; Nagai, Y. *J. Organomet. Chem.* **1977**, *128*, 173.
(29) Albrecht, J.; Richter, R.; Roewer, G. Patent DE 42 07 299 A1, 1993.
(30) Richter, R. Dissertation, Technischen Universität Bergakademie Freiberg, Germany, 1995.
(31) Richter, R.; Roewer, G.; Böhme, U.; Busch, K.; Babonneau, F.; Martin, H. P.; Müller, E. *Appl. Organomet. Chem.*, submitted.
(32) Massiot, D.; Thiele, H.; Germanus, A. *Bruker Rep.* **1994**, *140*, 43.

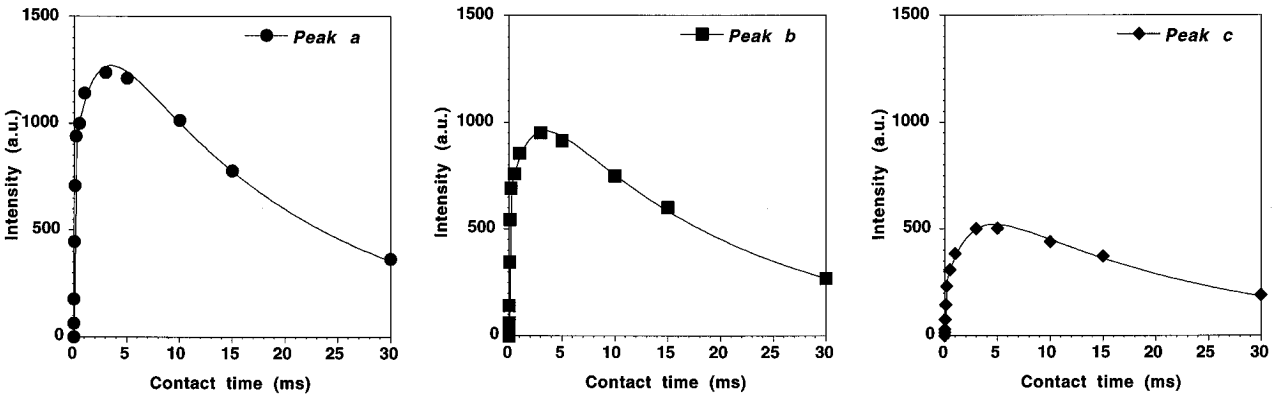

Figure 3. Evolution versus contact time of the ^{13}C CP MAS NMR signal intensities of the various peaks for the 180 °C MCPS. Curves were fitted with eq 4.

Table 1. Results Extracted from the ^{13}C CP and IRCP MAS NMR Spectra of the 180 °C MCPS

peak	C units	chemical shift (ppm)	LWHH[a] (ppm)	%[b]	T_{CH} (μs)	T_D (ms)	$T_{1\rho}^H$ (ms)	n
a	$MeSi(Si)_3$	−7.6	6	46	69	2.2	19	1.1
b	$MeClSi<$	4.1	6	35	67	2.1	19	0.9
c	$MeCl_2Si-$	11.4	2	19	118	2.4	22	0.5

[a] LWHH: line width at half-height. [b] The quantification was extracted from the fitted M_{0S} parameter.

all the IRCP spectra, the series of CP spectra was simulated with the same components.

The spectra were simulated with three peaks at −7.6 ppm (peak a), 4.1 ppm (peak b), and 11.4 ppm (peak c; Table 1). According to the NMR study performed on the oligosilanes,[26,27] they can be respectively assigned to methyl groups in tertiary or branched units, $MeSi(Si)_3$, linear units, $MeClSi<$, and terminal units, $MeCl_2Si-$. A small peak was introduced at 8.5 ppm, to simulate precisely the IRCP spectra, but its intensity is lower than 1% and will not be considered in the following discussion. It could be due to residual oligosilanes or $MeSiCl_3$ whose chemical shift is 9.7 ppm.[31] This example shows clearly how the analysis of IRCP spectra can provide very accurate simulations, even if peaks overlap. The integrated intensity for each peak of the CP spectra was plotted versus contact time (Figure 3). For the IRCP spectra, the integrated intensities were normalized and then plotted versus inversion time (Figure 4).

Two models exist to describe the spin dynamics associated with CP experiments.[18] The simplest model, called the I−S reservoir model, describes CP between two spin reservoirs, one for dilute spins, S, and one for abundant spins, I, and applies for S spins which are partially decoupled from the protons such as, for example, quaternary carbons. The magnetization can be expressed versus contact time with the well-known formula[33]

$$M_S(t_c) = \frac{\gamma_I}{\gamma_S} M_{0S} \frac{1}{1-\lambda}\left[1 - \exp\left(-(1-\lambda)\frac{t_c}{T_{IS}}\right)\right]\exp\left(-\frac{t_c}{T_{1\rho}^I}\right) \quad (2)$$

with $\lambda = T_{IS}/T_{1\rho}^I$.

M_{0S} is the magnetization at the equilibrium in the static field B_0, T_{IS} is the CP standard time which is related to the strength of the I−S dipolar coupling, and $T_{1\rho}^I$ is the relaxation time of the abundant spins in the rotating frame, that will cause a loss of magnetization for long contact time. γ_I and γ_S are the magnetogyric ratios for spins I and S, respectively.

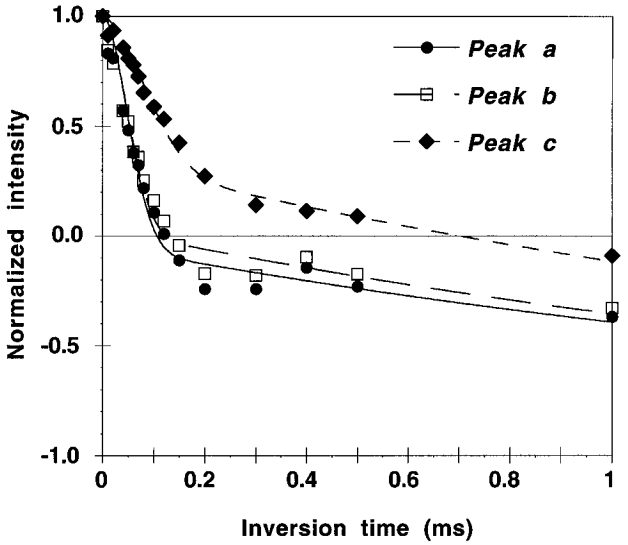

Figure 4. Evolution versus inversion time of the ^{13}C IRCP MAS NMR signal intensities of the various peaks for the 180 °C MCPS. Curves were fitted with eq 5.

It was found that the process of polarization inversion in the IRCP sequence has the same spin dynamics as the standard CP.[19] Thus, the S signal intensity can be expressed as a function of the inversion time, t_i as follows:

$$M_S(t_i) = M^0(t_c)\left[2\exp\left(-\frac{t_i}{T_{IS}}\right) - 1\right] \quad (3)$$

supposing $T_{IS} \ll T_{1\rho}^I$ and so $\lambda \ll 1$. $M^0(t_c)$ represents the polarized magnetization reached after the contact time, t_c. $T_{1\rho}^I$ is neglected because the spectra are usually recorded for inversion times lower than 1 ms. In this time range, relaxation with a characteristic time greater than 10 ms should not occur. For this I−S model, it is thus expected to observe in an IRCP experiment, a monoexponential decrease of the magnetization versus inversion time, with a constant rate T_{IS}.

In the second model called I*−I−S, the abundant spins are discriminated into two spin reservoirs I and I*, where the I spins are strongly dipolar coupled with the S spins, and the I* spins are weakly coupled. This model concerns, for example, rigid $^{13}CH_n$ groups. A quantitative expression for the polarized S magnetiza-

(33) Pines, A.; Gibby, M. G.; Waugh, J. S. *J. Chem. Phys.* **1973**, *59*, 569.

tion, in a standard CP experiment on ferrocene single crystals, has been given by Müller et al.[34] This formula was extended for powdered samples under moderate MAS as[16,35]

$$M_S(t_c) = \frac{\gamma_I}{\gamma_S} M_{0S}\left[1 - \frac{1}{n+1}\exp\left(-\frac{t_c}{T_D}\right) - \frac{n}{n+1}\exp\left(-\frac{3t_c}{2T_D}\right)\exp\left(-\frac{t_c^2}{T_{IS}^2}\right)\right]\exp\left(-\frac{t_c}{T_{1\rho}^I}\right) \quad (4)$$

T_{IS} is related to the strength of the I−S dipolar coupling. T_D is the spin diffusion constant and n is the number of directly coupled protons. Thus, for rigid SI_n groups, such as CH and CH_2, cross-polarization is not a single-exponential process but proceeds in two stages with different time scales: for typical organic compounds, the spin-diffusion time constant, T_D, is several hundred of microseconds, while T_{IS} is tens of microseconds. The same behavior is expected in an IRCP experiment, for the decrease of the magnetization during the inversion time:

$$M_S(t_i) = M^0(t_c)\left[\frac{2}{n+1}\exp\left(-\frac{t_i}{T_D}\right) + \frac{2n}{n+1}\exp\left(-\frac{3t_i}{2T_D}\right)\exp\left(-\frac{t_i^2}{T_{IS}^2}\right) - 1\right] \quad (5)$$

(neglecting again relaxation).

Typical examples of IRCP curves for various CH_n groups in sucrose have been already published[18] and clearly demonstrate the strength of this technique for differentiating rigid protonated C sites (CH and CH_2) whose polarization inversion occurs in a two-stage process and nonprotonated quaternary C atoms, which exhibit a monoexponential behavior. The dependence of eq 5 on the n value allows one even to distinguish between CH and CH_2 groups. The magnetization curves for these groups will present different turning points between the two regimes of polarization inversion for the normalized intensities at 0 and $-1/3$, respectively. Additionally, T_{CH} perfectly reflects the strength of the dipolar coupling, around ≈10−15 μs for rigid CH and CH_2 and usually greater than 300 μs for quaternary C.[18]

The behavior of spin dynamics during CP for CH_3 groups is more complex to predict, due to the fast internal motion of these groups that partially averages the effect of the strong dipolar coupling. In previous studies on CP and IRCP experiments, methyl groups have been analyzed in the frame of the I−S reservoir model, even if the increase or decrease of magnetization was not perfectly monoexponential versus time.[18,36] Recently, a clear two-stage character of cross polarization for methyl carbons was reported in the literature.[37] In the present MCPS, the polarization inversion of the methyl groups does not obviously follow a monoexponential law (Figure 4): a two-stage process seems to occur like in the I*−I−S reservoir model. But for rigid

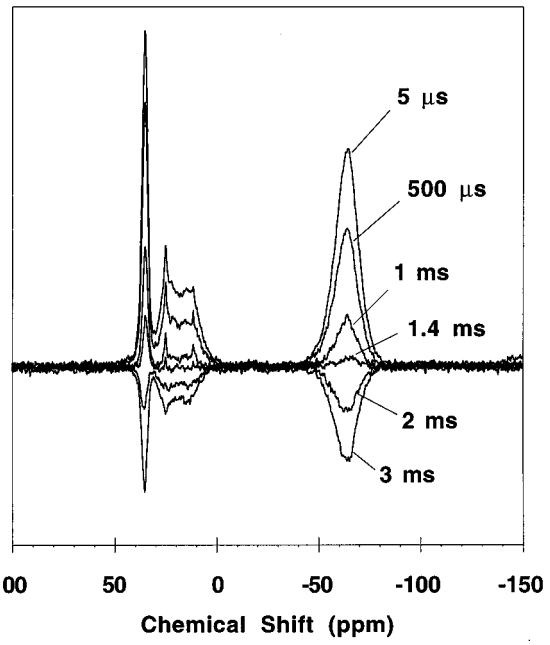

Figure 5. ^{29}Si IRCP MAS NMR spectra of the 180 °C MCPS (contact time 5 ms; inversion times are indicated for each spectra).

CH_3 groups, eq 5 predicts a turning point for the normalized intensity at $-1/2$, which is clearly not observed experimentally. To fit the polarization inversion curves, we have chosen to adjust three parameters in eq 5, not only the cross-polarization time T_{IS} and the spin diffusion time T_D but also n; n will be lower than 3, and this deviation could be indicative of mobility for the methyl groups.

The fitted curves for the ^{13}C IRCP MAS NMR experiments are presented in Figure 4 and the fitted parameters are summarized in Table 1. The agreement factors are quite good, greater than 0.98. The two peaks a and b have similar behaviors with $T_{CH} = 68 \pm 1$ μs and $T_D = 2.2 \pm 0.1$ ms. The n value, as expected, is lower than 3, $n = 1 \pm 0.1$. The peak c presents a much longer T_{CH} time, 118 μs, and a lower n value, 0.5. For CH_3 groups, the values are indeed very scattered in the literature from 100 to 500 μs, certainly due large variety of motions that such groups can exhibit.[36] The different behavior of peak c clearly indicates higher mobility for these terminal sites with a higher T_{CH} value and lower n value, due to a lower dipolar coupling. Then the variation of the ^{13}C CP-MAS signal intensities versus contact time t_c was fitted with eq 4. Analysis of these curves will allow us to quantify the various sites through the M_{0S} values. Five parameters should be fitted (T_{CH}, T_D, n, $T_{1\rho}^H$, M_{0S}), but three of them (T_{CH}, T_D, n) have already been extracted from the IRCP experiments, so only M_{0S} and $T_{1\rho}^H$ were fitted (Figure 3). The fitted parameters are listed in Table 1. All the agreement factors were greater than 0.96. $T_{1\rho}^H$ values are similar for the various sites, 20 ± 2 ms. From the M_{0S} values, quantification of the three different sites gave 46% of tertiary units (−7.6 ppm), 35% of linear units (4.1 ppm) and 19% of terminal units (11.4 ppm).

^{29}Si NMR Investigation. The series of ^{29}Si IRCP-MAS NMR spectra of MCPS 180 °C is presented in Figure 5. Three main domains are clearly observed: a broad signal around −64 ppm (chemical shift range for tertiary units), a composite signal between 10 and 30 ppm and a sharp signal at 35 ppm, certainly due to terminal

(34) Müller, L.; Kumar, A.; Baumann, T.; Ernst, R. R. *Phys. Rev. Lett.* **1974**, *32*, 1402.
(35) Alemany, L. B.; Grant, D. M.; Alger, T. D.; Zilm, K. W. *J. Am. Chem. Soc.* **1983**, *105*, 6697.
(36) Alemany, L. B.; Grant, D. M.; Pugmire, R. J.; Alger, T. D.; Zilm, K. W. *J. Am. Chem. Soc.* **1983**, *105*, 2133.
(37) Tekely, P.; Gérardy, V.; Palmas, P.; Canet, D.; Retournard, A. *Solid State Nucl. Magn. Reson.* **1995**, *4*, 361−367.

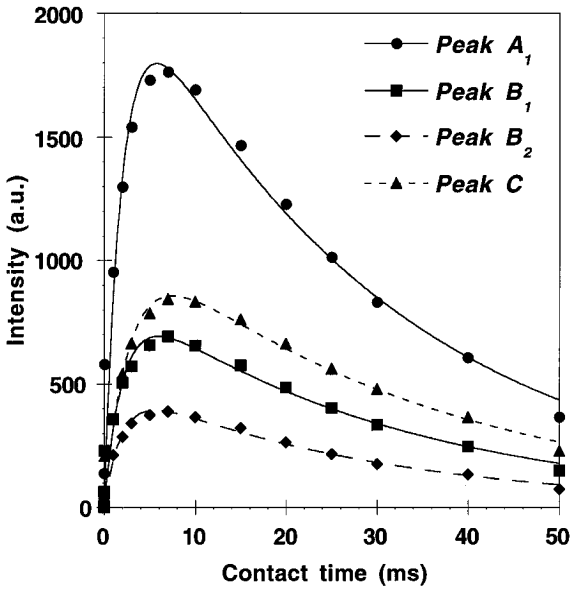

Figure 6. Evolution versus contact time of the ^{29}Si CP MAS NMR signal intensities of the various peaks for the 180 °C MCPS. Curves were fitted with eq 2.

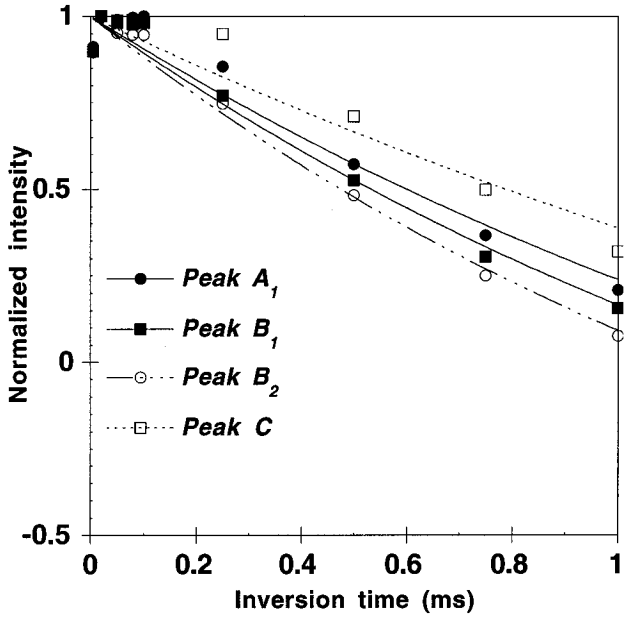

Figure 7. Evolution versus inversion time of the ^{29}Si IRCP MAS NMR signal intensities of the various peaks for the 180 °C MCPS. Curves were fitted with eq 3.

Table 2. Results Extracted from the ^{29}Si CP and IRCP MAS NMR Spectra of the 180 °C MCPS (Abbreviations as in Table 1)

peak	chemical shift (ppm)	LWHH (ppm)	%	T_{SiH} (ms) (from CP)	$T_{1\rho}^{H}$ (ms)	T_{SiH} (ms) (from IRCP)
A_1	−64.0	13	46	2.0	30	2.1
D	−51.2	9	3	1.9	26	
	11.3	1	<1			
B_1	14.1	12	18	2.0	31	1.8
B_2	24.2	8	10	1.9	29	1.7
	25.1	1	1			
C	35.3	3	22	2.7	34	2.7

units. The times for the inversion of the peaks range from 1.4 to 2.0 ms. The peak that inverts the last is due to the terminal units at 35 ppm. The simulations of the CP and IRCP spectra were done in a way similar to that followed for the ^{13}C NMR spectra. The IRCP spectra were first simulated to identify the various peaks. The spectra were fitted with 7 peaks (Table 2). The broad signal due to tertiary units was mainly simulated with one peak A_1 at −64.0 ppm. It was necessary to add a minor peak at −51.2 ppm (peak D) to account for the dissymetry observed at low field. The simulation of the composite signal between 10 and 30 ppm was more difficult because of the presence of several overlapping signals as revealed by the inversion behavior of the peaks in the IRCP. Two sharp minor peaks are present at 11.3 ppm and at 25.1 ppm: they can be clearly seen for $t_i = 1$ ms. Two major broader peaks were identified at 14.1 ppm (peak B_1) and at 24.2 ppm (peak B_2). The sharp signal due to terminal units could be simulated with one unique peak at 35.3 ppm (peak C). The variation of the integrated intensity of the major peaks of the CP spectra, versus contact time is shown in Figure 6. The variation of the normalized integrated intensities from IRCP experiments is shown in Figure 7 versus inversion time.

In the present sample, no protons are directly bonded to Si: the nearest protons are in Si−CH_3 groups. The dynamics of cross-polarization and polarization inversion can be safely described by using the conventional I−S reservoir model (see above). In this case, the CP and IRCP behaviors can be fitted with eqs 2 and 3, respectively. The two sets of experiments were fitted independently. The fitted curves obtained for the CP dynamics are shown in Figure 6. The agreement between experimental and calculated curves is very good, showing that the application of the I−S reservoir model seems quite valid for the present system. The IRCP curves were fitted for inversion times ≤1 ms, so that $t_i \ll t_c$ (Figure 7). The fitted parameters are summarized in Table 2 for each resonance peak.

The T_{SiH} values are long compared to the observed T_{CH} values, because of a much lower dipolar coupling. The values found from CP and IRCP experiments, are in very good agreement, around 2.0 ± 0.2 ms for the major peaks, A_1, B_1, and B_2 at −64.0, 14.1, and 24.2 ppm. For the peak C at 35.3 ppm due to terminal units, $MeCl_2Si$−, a higher value is observed, 2.7 ms, which should reveal higher mobility for these groups as already observed for the ^{13}C experiments. The $T_{1\rho}^{H}$ values are quite similar for the various sites, 30 ± 5 ms. The minor sharp ^{29}Si resonance peaks at 11.3 and 25.1 ppm are certainly due to some residual silanes of low molecular weight, such as methylchlorosilane (δ = 12.2 ppm).[31]

Comparison between ^{29}Si and ^{13}C NMR Results. The main objective of the NMR study on the 180 °C MCPS was to show how detailed structural information can be extracted from ^{13}C and ^{29}Si spectra, using both CP and IRCP techniques. Analysis of a series of CP and IRCP spectra permits one to get accurate simulations and thus to extract the characteristic parameters of the various resonance peaks (chemical shift, line width), as well as their intensities. A comparison of the results obtained from ^{13}C and ^{29}Si experiments are summarized in Table 3 for the major peaks. The peaks can be assigned by comparison with the liquid NMR study performed on the oligosilanes.[26,27] One problem is the assignment of the peak B_2 at 24.2 ppm, which could be due to either linear or terminal groups. Comparison of the quantitative analysis for both nuclei seems to show that this peak is due to linear units with the corresponding ^{13}C resonance peak b at 4.1 ppm. In addition, the parameters which characterized the dynamics of

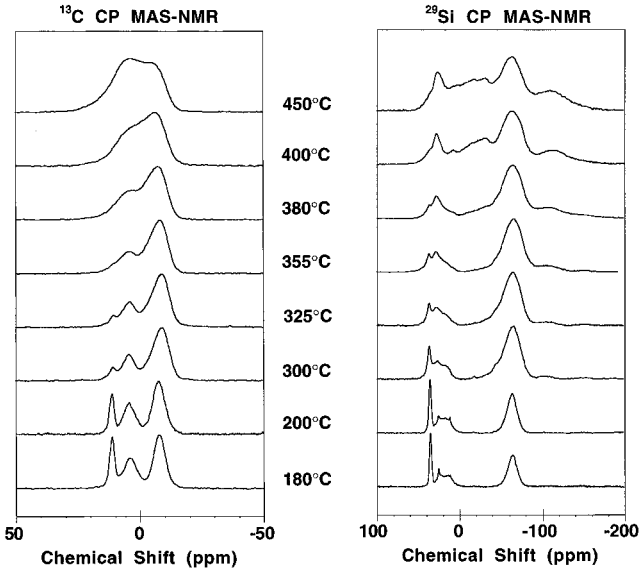

Figure 8. Evolution of the ^{13}C and ^{29}Si CP MAS NMR spectra of the samples heated from 180 to 450 °C (respective contact times 3 and 10 ms).

Table 3. Comparison between ^{29}Si and ^{13}C NMR Data on the 180 °C MCPS and Tentative Assignments (Peak Labels in Parentheses)

^{13}C NMR		^{29}Si NMR		
chemical shift (ppm)	%	chemical shift (ppm)	%	assignments
−7.6 (*a*)	46	−64.0 (A_1)	46	$MeSi(Si)_3$
		−51.2 (D)	3	$(-CH_2)Si(Si)_3$
4.1 (*b*)	35	14.1 (B_1)	18	MeClSi<
		24.2 (B_2)	10	
11.4 (*c*)	19	35.3 (C)	23	$MeCl_2Si-$

polarization transfer between the various spin systems can help in such assignments: the characteristic T_{SiH} time for the peak B_2 at 24.2 ppm (1.9 ms) is very close to that found for the peak B_1 at 14.1 ppm (2.0 ms) and much lower than that found for the peak C at 35.3 ppm (2.7 ms), which is due unambiguously to terminal groups. For such terminal groups of high mobility, the dipolar coupling is averaged to a larger extent than for the other sites, linear and tertiary, and this is clearly seen in the T_{SiH} and moreover in the T_{CH} values. The presence of two resonance peaks assigned to linear groups will be discussed later.

Another problem is the assignment of the minor peak D at −51.2 ppm: its chemical shift is in the range of tertiary units, but such downfield values were not found in the liquid NMR study performed on the oligosilanes, for which all the values range from −60 to −67 ppm.[26,27] It was thus suggested, in agreement with the TG/MS results that will be presented later, that this peak could be due to the formation of carbosilane units, $(-CH_2)$-$Si(Si)_3$. If this is true, one can wonder why the ^{13}C resonance peak due to CH_2 groups was not found in the ^{13}C NMR experiments. Indeed according to the quantification done for the various ^{29}Si sites and reported in Table 2, the ratio CH_2/CH_3 will be very low, <3%, and the corresponding peak could be difficult to identify. The problem of detection of the various ^{13}C resonances will be discussed later.

III.2. NMR Characterization of Samples Heated from 180 °C to 450 °C. Figure 8 represents the ^{13}C and ^{29}Si CP MAS NMR spectra of nine samples prepared at reaction temperatures ranging from 180 to 450 °C and recorded with respective contact times of 3 and 10 ms. Above 300 °C, the ^{13}C resonance signals strongly broaden, and new signals at lower field appear for $T \geq 355$ °C. But all the signals strongly overlap, and a direct identification of the various signals is not possible.

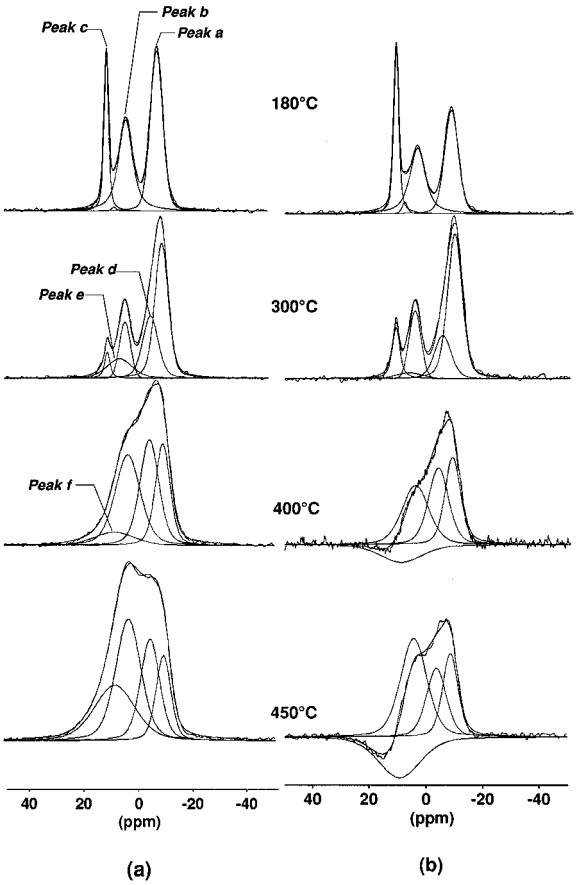

Figure 9. Experimental and simulated ^{13}C CP (a) and IRCP (b) MAS NMR spectra of samples heated to 180, 300, 400, and 450 °C. (a) $t_c = 3$ ms; (b): $t_c = 3$ ms, and $t_i = 50$ μs.

One advantage of ^{29}Si NMR compared to ^{13}C NMR for these particular samples is the extended chemical shift range, as shown in Figure 8. It should allow an easy assignment of the peaks based on their chemical shift values. The principal modification of the spectra, besides a general broadening of all the peaks, is clearly the presence of new peaks between 0 and −50 ppm for $T \geq 380$ °C, whose intensities increase with reaction temperature. $Si(C_4)$ units, such as in poly(carbosilane), are characterized by resonance peaks at around 0 ppm.[9] As shown previously, peaks due to tertiary $MeSi(Si)_3$ units in polysilanes have quite a different chemical shift, at around −60/−70 ppm. So new peaks between 0 and −60 ppm could be due to the polysilane-to-polycarbosilane transformation that will occur through a progressive substitution of Si−Si by Si−C bonds (formation of (Si−CH_2−Si) sites), generating various $Si(Si_x)(C_{4-x})$ mixed units ($0 \leq x \leq 3$).

Series of ^{13}C and ^{29}Si MAS NMR spectra using CP and IRCP sequences have been recorded on these nine samples and analyzed in detail to identify and quantify the various ^{13}C and ^{29}Si sites present in these various samples.

^{13}C NMR Investigation. Examples of CP spectra (contact time 3 ms) and IRCP spectra (contact time 3 ms; inversion time 50 μs) are presented in Figure 9 for the 180, 300, 400, and 450 °C samples. The dynamics of polarization-inversion seems quite different between

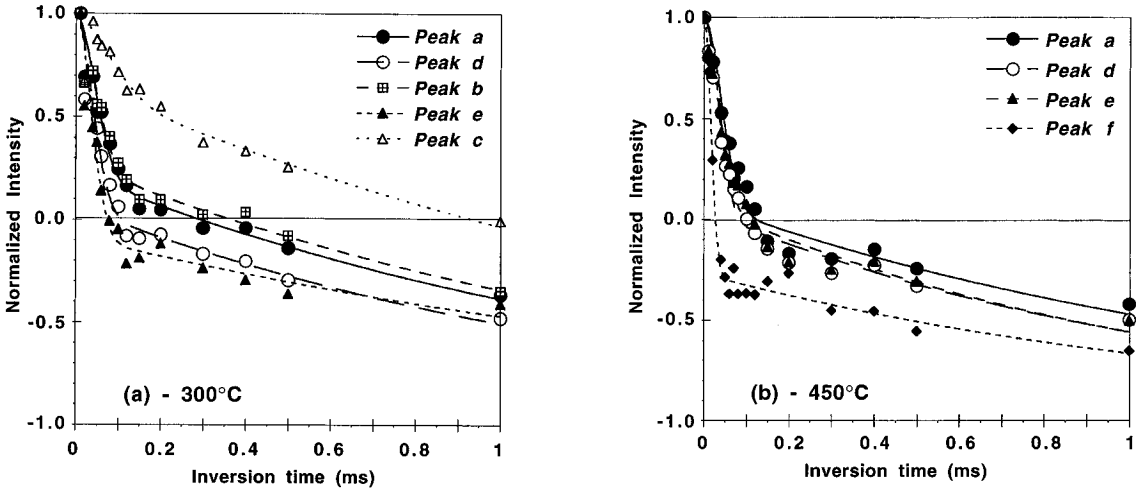

Figure 10. Fitted curves for the ^{13}C IRCP data of (a) the 300 and (b) 450 °C sample. Curves were fitted with eq 5.

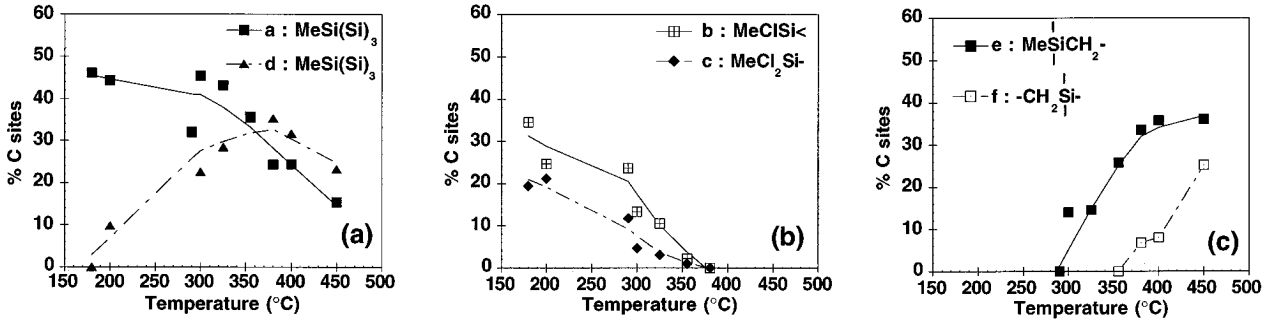

Figure 11. Evolution versus temperature of the percentage of each C sites: (a) tertiary silane units (peaks a and d); (b) terminal (peak b), and linear (peak *c*) silane units; (c) carbosilane units (peaks e and f).

the samples. For $t_i = 50$ μs, all the peaks are positive for the 180 and 300 °C sample, while one signal is already negative in the 400 and 450 °C samples.

All the spectra have been simulated following the procedure previously described for the 180 °C MCPS (Figure 9). The IRCP spectra were first simulated, and then the set of peaks derived was used to simulate the CP spectra. The results obtained for a sample were always used as starting points to simulate the spectra of the sample heat treated to a temperature immediately higher. Six peaks, indicated in Figure 9 and labeled a−f, were used to simulate all the series of CP and IRCP spectra. As previously described, three peaks due to tertiary units (peak a), linear units (peak b), and terminal units (peak c) are present in the spectra of the 180 °C MCPS. At 200 °C, an additional peak at −6.2 ppm (peak d) appears. Then above 300 °C, another new peak at 6.5 ppm, (peak e) is added, broader than the previous one. At 380 °C, the two peaks a and b have disappeared, but a new peak at 9.3 ppm is now present (peak f) with an even larger line width, 17 ppm instead of 5−10 ppm. The chemical shift values do not vary greatly with the reaction temperature.

The evolution of the peak intensities versus contact time in the CP experiments, or versus inversion time in the IRCP experiments were fitted for each temperature, following the same procedure previously described for the 180 °C MCPS. Examples of curves fitted with eq 5 for the IRCP data of the 300 and 450 °C samples are presented in Figure 10 for the 300 °C sample, the peaks a−c due to CH_3 groups in tertiary, linear, and terminal units have similar behavior to what was found for the 180 °C MCPS. The new peaks, d and e, invert for shorter t_i, around 0.1 ms. The corresponding curves have been correctly fitted with eq 5 with T_{CH} around 50−55 μs, characteristic of CH_3 groups. The slightly lower T_{CH} than for the peaks a and b ($T_{CH} \approx 65$ μs) should suggest that these peaks are associated with CH_3 groups with lower mobility. For the 450 °C sample (Figure 10b), the peaks b and c due to linear and terminal units have disappeared. The peaks a, d, and e present quite similar behavior characteristic of methyl groups with similar dynamics ($T_{CH} \approx 50-55$ μs). But the most important point is the new peak f which exhibits a totally different inversion behavior, as clearly seen in Figure 9. It inverts much faster for 20 μs $\leq t_i \leq$ 40 μs (Figure 10b), and such values are characteristic of CH or CH_2 groups.[18] The inversion curve shows clearly a change in the two regimes around $-1/3$ and not around 0, indicating that the corresponding groups should be rigid CH_2 groups. Indeed, the curve was successfully fitted with eq 5 and $n = 2$, and gives $T_{CH} = 24$ μs. It is thus totally clear that CH_2 groups are formed at this reaction temperature.

Besides the peaks a ($MeSi(Si)_3$), b ($MeClSi<$), and c ($MeCl_2Si-$) found in the MCPS, new peaks d and e are thus assigned to CH_3 groups, while peak f which appears at 380 °C is assigned to CH_2 groups. The percentages of each C sites were calculated from the M_{0S} magnetization values and extracted from the CP data, and their evolution versus reaction temperature is presented in Figure 11.

The chemical shift values of peak d (−7/−9 ppm) are typical of tertiary units, $MeSi(Si)_3$. Its intensity (Figure 11a) is related to a decrease in intensity of peaks b and c (Figure 11b), thus to a consumption of terminal and linear units. This new peak could correspond to the formation of more cross-linked structures which in-

Table 4. Proposed Assignments for the Various ^{13}C Resonance Peaks

peak	chemical shift range (ppm)	assignment	peak	chemical shift range (ppm)	assignment
a	−7 to −9	*Me*Si(Si)$_3$	d	−4 to −6	*Me*Si(Si)$_3$
b	3 to 4	*Me*ClSi<	e	4 to 6	MeSiCH$_2$—
c	11	*Me*Cl$_2$Si−	f	9	—Si—CH$_2$—

volved cyclization reactions. Such a mechanism will be presented in the discussion.

Above 300 °C, peak e assigned to methyl groups appears (Figure 11c). Its chemical shift is quite different from the chemical shifts of peaks a and d which are typical of tertiary units in polysilane backbone. The chemical shift of peak e varies from 6.5 ppm in the 300 °C sample to 4.4 ppm in the 450 °C sample, and these values have already been found for methyl groups in poly(carbosilane) units.[9] But a poly(carbosilane) backbone implies the presence of both CH_3 and CH_2 units, and in the present case, CH_2 groups are clearly identified only in the 380 °C sample. The chemical shift value for these methylene groups (9.3 ppm) is consistent with CH_2 groups in poly(carbosilane) units.[38] A possible explanation for this apparent discrepancy is that methylene groups do exist between 325 and 380 °C, but in low amount, and indeed this will be confirmed by the following ^{29}Si NMR study. The associated peak can not be clearly identified through the analysis of the ^{13}C NMR spectra. Moreover, when detected, the peak is quite broad (15−20 ppm), characteristic of a rather large distribution of methylene sites and lies underneath the other components. This clearly points out some limits in such an analysis due to the short chemical shift range for the ^{13}C resonance peaks which strongly overlap, especially if they are broad. Proposed assignments for the various ^{13}C resonances are summarized in Table 4.

^{29}Si NMR Investigation. According to the previous conclusions regarding the ^{13}C NMR investigation, several points will be discussed in the following ^{29}Si NMR study:

(i) Formation of carbosilane units: the ^{13}C IRCP NMR experiments were essential to clearly identify the formation of methylene groups. In the ^{29}Si experiments, the $^1H-^{29}Si$ dipolar coupling should not be so different for silane or carbosilane units, even if a larger amount of protons as second neighbors in carbosilane units and a possible reduced mobility, should cause a decrease in the cross-polarization time, T_{SiH}, of these carbosilane units compared to silane units. This will be discussed in the following paragraph.

(ii) Formation of Si−H bonds: if carbosilane units are formed through "Kumada-rearrangement" the formation of Si−H bonds is expected (eq 6): But the identification

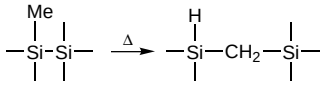

(6)

of Si sites with Si−H bonds based on chemical shift considerations will not be easy in the present study, because the corresponding peaks will certainly overlap

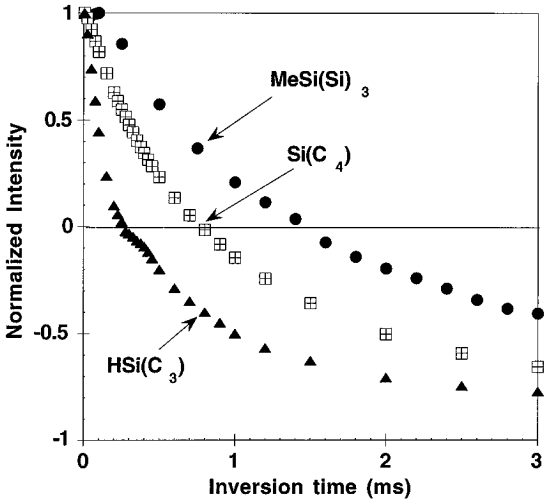

Figure 12. Variation versus inversion time in ^{29}Si IRCP MAS NMR experiments of the signal intensities of SiC_4 and $HSiC_3$ units in the Yajima poly(carbosilane). For comparison, the behavior of the signal due to tertiary silane units, MeSi(Si)$_3$ is indicated (contact time 5 ms).

with others. The IRCP technique can be of great help, because the behavior of Si units with a proton directly bonded should be totally different from the behavior of Si units with no Si−H bonds. They should exhibit the same differences than a CH group and a quaternary C in ^{13}C IRCP experiments.

As already mentioned, there is a lack of data in the literature on ^{29}Si IRCP NMR spectra. A study published on amorphous hydrogenated silicon did not provide a detailed analysis.[24] Spectra of a commercially available poly(carbosilane) prepared according to Yajima procedure[39] were thus recorded. The ^{29}Si NMR spectrum presents two peaks one due to *Si*(C$_4$) units at 0 ppm and one due to H*Si*(C$_3$) units at −17 ppm.[9] Polarization inversion behaviors are obviously quite different for the two sites (Figure 12): the curve corresponding to the *Si*(C$_4$) site exhibits a classical monoexponential behavior that can be fitted according to eq 3, and leads to $T_{SiH} = 1.1$ ms. For the H*Si*(C$_3$) sites, a two-stage regime is observed with a turning point around 0, characteristic of a ^{29}SiH group. The T_{SiH} value extracted according to eq 5 with $n = 1$, is much shorter, 150 μs. IRCP experiments should thus allow identification of sites with Si−H bonds, if they are in appreciable amounts. Moreover, these results on the Yajima precursor provide a reference for the behavior of carbosilane *Si*(C$_4$) units in ^{29}Si IRCP NMR experiments. T_{SiH} is shorter (1.1 ms) than for tertiary units in the 180 °C MCPS (2 ms) as shown in Figure 12. So a discrimination between polysilane and poly(carbosilane) units based on IRCP behavior seems possible.

Examples of CP spectra (contact time 10 ms) and IRCP spectra (contact time 10 ms; inversion time 1 ms) are presented in Figure 13 for the 180, 300, 355, and 400 °C samples. Differences are clearly seen for an inversion time of 1 ms: in the 180 and 300 °C samples, all the peaks are positive as expected for polysilane units, while in the 400 °C samples the new peaks between 0 and −50 ppm are already negative, strongly suggesting the presence of poly(carbosilane) units.

(38) Wu, H.-J.; Interrante, L. V. *Chem. Mater.* **1989**, *1*, 564.

(39) Yajima, S.; Hasegawa, Y.; Hayashi, J.; Iimura, M. *J. Mater. Sci.* **1978**, *13*, 2569.

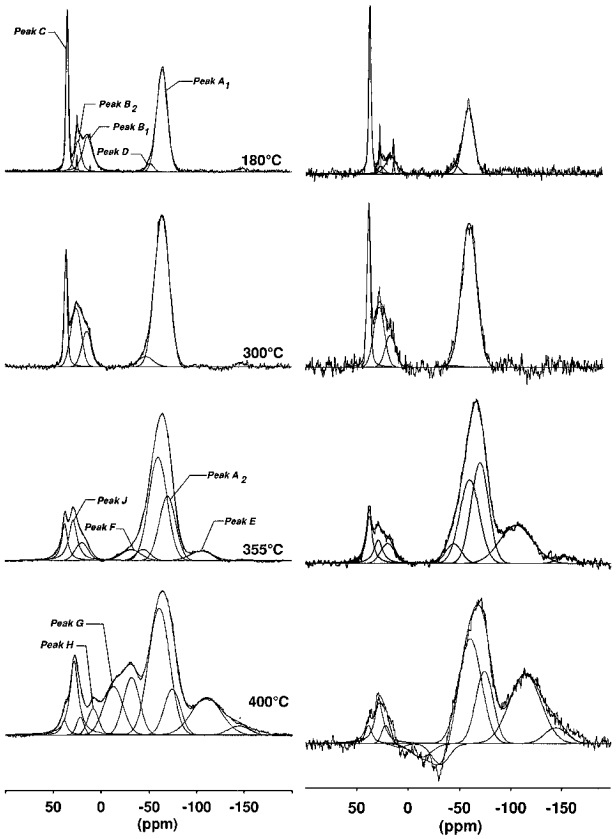

Figure 13. Experimental and simulated ^{29}Si CP (a) and IRCP (b) MAS NMR spectra of samples heated to 180, 300, 355, and 400 °C. (a) t_c = 10 ms; (b) t_c= 10 ms, and t_i = 1 ms.

The CP and IRCP spectra of the 180, 200, 300, 355, and 400 °C samples have been simulated and examples of simulations are given in Figure 13. The main peaks found in the 200−300 °C reaction temperature range are similar to those already found for the 180 °C MCPS: main peak A_1 around −64 ppm due to tertiary units (Me*Si*(Si)$_3$), two components, B_1 and B_2 around 14 and 25 ppm due to linear units (MeCl*Si*<), peak C around 36 ppm due to terminal units ($MeCl_2Si-$) and peak D around −50 ppm tentatively assigned to carbosilane ($-CH_2$)Si(Si$_3$) units. In the 325 °C sample, new peaks appear: peak E at −105 ppm and peak F at −32 ppm. In the 400 °C sample, additional peaks are present, peak A_2 at −60 ppm, peak G at −12 ppm and peak H at 8 ppm. The variations of the normalized intensities of peaks A_1, E, F, G, and H extracted from the IRCP spectra are presented in Figure 14 for the 400 °C sample chosen as a representative example. They show clearly a difference in the dynamics of polarization inversion for the three peaks F, G, and H which invert faster than peak A_1. Indeed, they exhibit behavior similar to that found for the Si(C_4) units in the Yajima poly(carbosilane). Interestingly peak E inverts slower that peak A_1, suggesting a poorly protonated environment for the corresponding Si site. For the 200, 300, 355, and 400 °C samples, the polarization inversion curves have been fitted with eq 3, for $t_i \leq 1$ ms, to extract the T_{SiH} values. The variations versus contact time, of the intensity of the peaks in the ^{29}Si CP NMR spectra were also fitted with eq 2 mainly to extract quantitative data concerning the various Si sites. Analysis of the CP spectra shows that quantitative data can be directly extracted with reasonable accuracy, from the simulation of the spectrum recorded with 10 ms contact

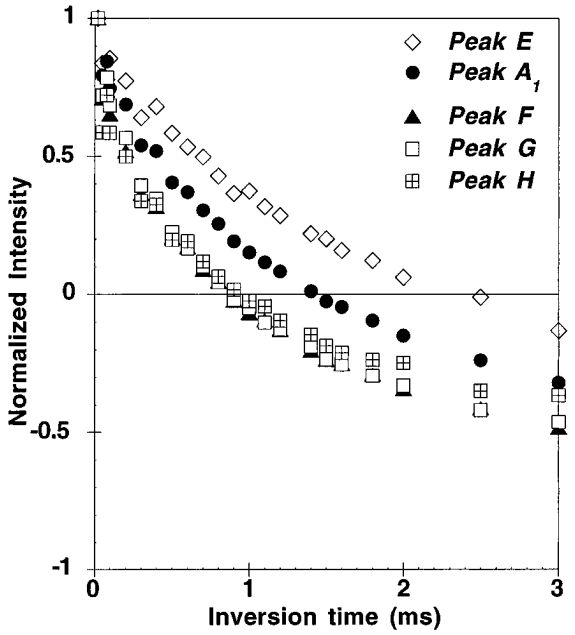

Figure 14. Variation versus inversion time in ^{29}Si IRCP MAS NMR experiments of the intensities of peaks A_1, E, F, G, H in the 400 °C sample (contact time 5 ms).

time. This was done for the 220, 300, 325, 380, and 450 °C samples to obtain additional data.

Up to 300 °C, no new peaks are present besides those already found in the 180 °C sample. The number of tertiary units (peak A_1) regularly increases from 46% to 57%, while the number of terminal groups (peak C) decreases from 23% to 12%. The number of linear units (peaks B_1 and B_2) remains almost constant around 25%. As for the minor peak D assigned to carbosilane units, its intensity remains low <6%. In the 300 °C sample, new peaks are clearly present, at −105, −60/−70, and −32 ppm.

Peak E at −105 ppm is characterized by a long T_{SiH} characteristic time, $T_{SiH} \approx 4$ ms (Figure 14), which indicates a poorly protonated environment. This chemical shift is typical for silica sites which would indicate that oxidation of the sample has occurred. But all of the experiments have been performed under strictly controlled inert atmosphere preventing any hydrolysis of the Si−Cl bonds to occur. Indeed the intensity of this peak is increasing continuously from 355 to 450 °C and is not present in the lower temperature samples. Moreover, in samples heat treated at 750 °C, the intensity of this peak drastically decreases. Examination of published data for $[(Me)_3Si]_{4-x}Si(Me)_x$ silanes with $0 \leq x \leq 4$ shows chemical shift values of 0 ppm for $x = 4$ (Me_4Si), −19.7 ppm for $x = 3$ (Me_3Si(Si)), −48.7 ppm for $x = 2$ ($Me_2Si(Si)_2$), −87.9 ppm for $x = 1$ (Me*Si*(Si)$_3$) and −135.5 ppm for $x = 0$ (*Si*(Si$_4$)).[40] The reported values for tertiary units in methylchlorooligosilanes are around −60/−65 ppm.[27,28] The 20−30 ppm lowfield shift is certainly related to differences in environments of the first Si neighbors. It is thus expected that in MCPS, quaternary units *Si*(Si)$_4$ will be characterized by a chemical shift around −105/−115 ppm. It seems thus very likely that peak E corresponds to the formation of quaternary Si units, Si(Si$_4$), in

(40) Marsmann, H. In *NMR Basic principles and Progress*; Dielh, P., Fluck, E., Kosfeld, R., Eds.; Springer Verlag: Heidelberg, 1981; Vol. 17.

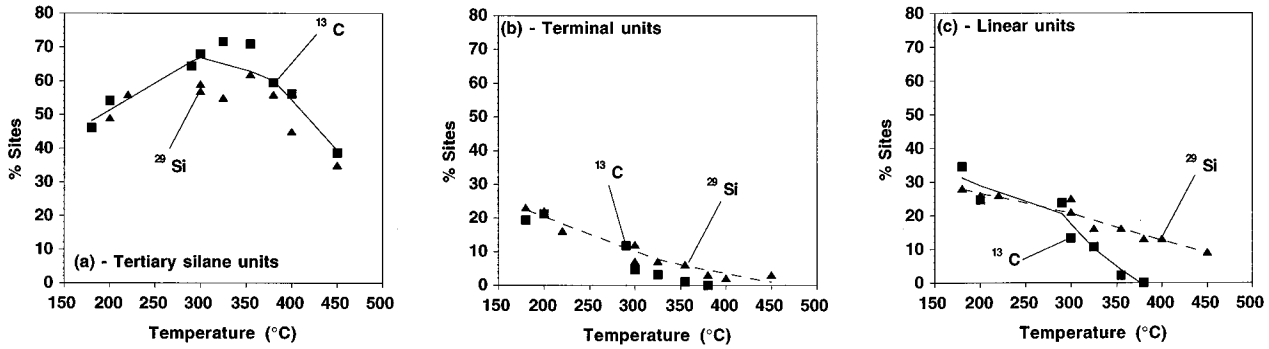

Figure 15. Comparison between ^{29}Si and ^{13}C NMR results: (a) tertiary units $MeSi(Si)_3$ (^{29}Si peaks $A_1 + A_2$; ^{13}C peak a); (c) linear units (^{29}Si peaks $B_1 + B_2 + J$; ^{13}C peak b) and (b) terminal units (^{29}Si peak C; ^{13}C peak c).

Table 5. Proposed Assignments for the ^{29}Si Resonance Peaks

peak	chemical shift range (ppm)	assignments
A_1/A_2	−60 to −70	tertiary units $MeSi(Si)_3$
B_1/B_2	15 to 30	linear units $MeClSi<$
C	35 to 40	terminal units $MeCl_2Si-$
D	−45 to −50	carbosilane units $(-CH_2)Si(Si)_3$
E	−105 to −110	quaternary units $Si(Si)_4$
F	−30 to −35	carbosilane units, $(-CH_2)_xMe_{2-x}Si<(x = 1, 2)$
G	−10 to −15	carbosilane units, $(-CH_2)_xMe_{3-x}Si-(x = 2, 3)$
H	0 to 10	carbosilane units, $(-CH_2)_xMe_{4-x}Si(x = 3, 4)$
J	25 to 30	carbosilane units, $(-CH_2)MeClSi-$

perfect agreement with its behavior during polarization inversion experiments.

Two peaks in the chemical shift range of tertiary units are now present at −60 ppm (peak A_1) and −70 ppm (peak A_2). A quantitative comparison between the number of tertiary units extracted from the ^{13}C experiments (peaks a and d) and the present data shows that they are indeed due to tertiary $MeSi(Si)_3$ units (Figure 15a). Peak F at −31.8 ppm is in the chemical shift range expected for carbosilane units, $(-CH_2)_{2-x}Me_xSi<$ ($x = 0.1$). Moreover, it is characterized by a short T_{SiH} value (1.1 ms) which strengthens its assignment to proton-rich carbosilane units. The reported chemical shift value for $[Me_3Si]_2Si(Me)_2$ is −48.7 ppm, as already mentioned.

Three peaks B_1, B_2, and C are attributed to Si−Cl-containing units. The assignment of peak C to terminal $MeCl_2Si-$ units is unambiguous based on chemical shift values, and comparison with ^{13}C results (peak c, Figure 15b). Peaks B_1 and B_2 could be first assigned to linear $MeClSi<$ units. The sum of the intensities of these peaks was compared with the intensity of the ^{13}C peak b due to linear units (Figure 15c). Up to 300 °C, the two curves are quite similar, suggesting that peaks B_1 and B_2 are due to linear units. Above this temperature, the intensity of these peaks does not follow the same evolution as peak b, strongly suggesting that peaks B_1 and/or B_2 are not only related to these units in this temperature range. Indeed the quantitative evolution of peak B_1 above 300 °C, is very similar to that of peak b, suggesting that peak B_1 is due to linear units, while peak B_2 is now due to other units. For clarity, it will be called peak J. It is characterized by a short T_{SiH} time (1.5 ms) compared to the other two and could also be due to carbosilane units, such as $(-CH_2)MeClSi-$. A chemical shift value of 26.8 ppm has been reported for Me_2ClSi- units in methylchlorooligosilanes.[27]

In the 400 °C sample, additional peaks are now present at −12.8 ppm (peak G) and 8.2 ppm (peak H). They are also characterized by short T_{SiH} values (1.1−1.2 ms) typical of proton-rich carbosilane units in

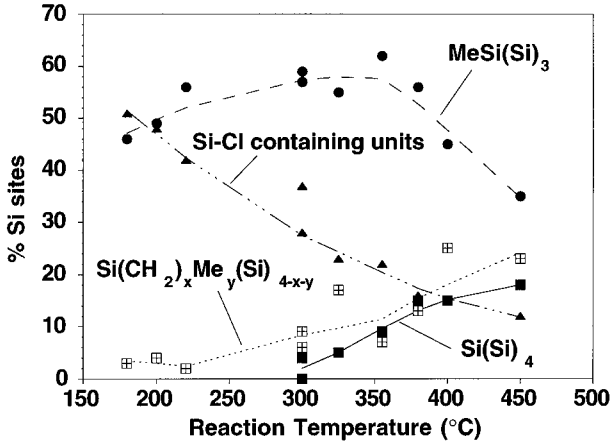

Figure 16. Evolution of the percentages of the various Si sites, tertiary silane units [$MeSi(Si_3)$], quaternary silane units [$Si(Si_4)$], carbosilane units [$(-CH_2)_xMe_ySi(Si)_{4-x-y}$] and Si−Cl-containing sites extracted from the ^{29}Si NMR study.

agreement with their chemical shift range. Similar peaks are also found in the spectra of the 450 °C sample with a large increase in intensity for peak H. Peak G could thus be assigned to carbosilane $(-CH_2)_xMe_{3-x}Si-$ ($x = 2, 3$) units, while peak H could be due to carbosilane $(-CH_2)_xMe_{4-x}Si$ ($x = 3, 4$) units.

This analysis shows clearly the presence above 355 °C of carbosilane units, in various environments whose number increases with temperature. However a precise description of these units is very difficult due to a lack of references. None of the detected peaks shows very short T_{SiH} values due to the presence of Si−H bonds; such species should not thus exist in appreciable amount in the samples. Tentative assignments of the peaks A−J are summarized in Table 5. Estimations of the amounts of silane units ($MeSi(Si)_3$ (peaks A_1, A_2) and $Si(Si)_4$ (peak E)), Si−Cl containing units (peaks B_1, B_2, C, J) and carbosilane units, $(-CH_2)_yMe_xSi(Si)_{4-x-y}$ (peaks F, G, H) are reported in Figure 16.

III.3. TG/MS Study of the MCPS 220 °C. To obtain additional information on the mechanism of the

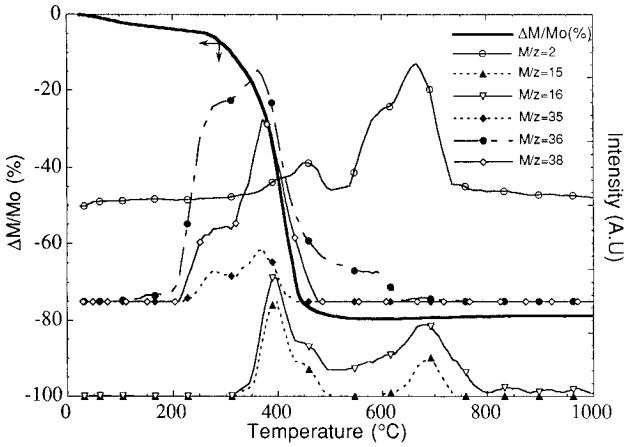

Figure 17. TG/MS curves recorded on the 220 °C MCPS.

polysilane−poly(carbosilane) transformation, a thermogravimetric analysis coupled with mass spectrometry (TG/MS) was performed on the 220 °C MCPS up to 1000 °C. The results are shown in Figure 17. The total weight loss is 80%. A theoretical weight loss can be crudely estimated from the chemical analysis, $MeSiCl_{0.49}$, assuming the formation of SiC. Two simple assumptions can be made on the Cl-containing gaseous species, HCl or $MeSiCl_3$, leading respectively to 34% and 47%. This strongly suggests the loss of additional oligosilanes during the pyrolysis. The weight loss occurs in one main step from 200 to 450 °C, where HCl and CH_4 are detected. Evolution of HCl (m/z = 35, 36, and 38) clearly occurs in two stages, from 200 and 300 °C, and from 300 and 450 °C. During this last stage, CH_4 (m/z = 15, 16) and H_2 (m/z = 2) are also formed. At higher temperatures, CH_4 and H_2 are still generated in various stages, from 450 to 500 °C and then from 550 to 800 °C. Extreme care was taken to carry out the experiment in an oxygen and moisture free atmosphere. No water (m/z = 18) was detected that could be due to hydrolysis.

IV. Discussion

IV.1. Formation of Methylchloropolysilanes (180 °C). The methylchlorooligosilanes **3**−**7** can be considered as "building blocks" of highly cross-linked methylchloropolysilane networks, whose structures were largely unknown so far. Even less investigated was the cross-linking itself.

The complementary use of IRCP and CP techniques for ^{13}C and ^{29}Si NMR investigation allows one to identify and quantify the various silane sites present in the MCPS samples. ^{29}Si and ^{13}C NMR data for MCPS 180 °C (Table III) give the following chemical composition, $SiMeCl_{0.73}$, which is in reasonably good agreement with the reported elemental analysis, $MeSiCl_{0.62}$.[30] A cross linking degree of C.D. = 2.27 ± 0.05 can also be calculated according to

$$\text{C.D.} = [3 \times \%(\text{MeSi(Si)}_3) + 2 \times \%(\text{MeClSi<}) + \%(\text{MeCl}_2\text{Si}-)]/100 \quad (7)$$

The C.D. value represents the number of Si−Si bonds per Si. A value above 2 indicates the presence of cyclic polymer structures, while a smaller value corresponds to the formation of exclusively branched Si backbones.

The average Cl/Si molar ratio of the oligosilane mixture obtained at 175 °C is 1.45. Its drastic decrease

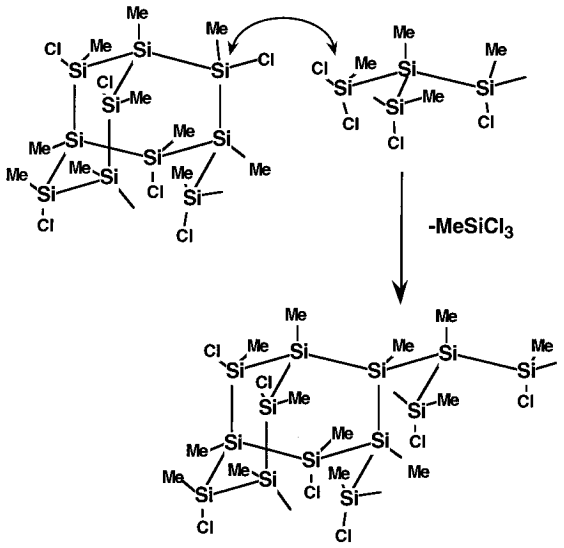

Figure 18. Proposed structure for 180 °C MCPS.

to 0.62 at 180 °C (2 h) is caused by enhanced cross-linking reactions leading to the evolution of the monosilane $MeSiCl_3$ as a gaseous cross-linking product. The Si−Cl bonds of the polymer backbone are replaced by Si−Si bonds. Due to the parent functionality of 2 Cl per Si the backbone growth is governed by the formation of branch points (tertiary Si atoms) **8**, which are obviously obtained in a two-step process:

(1) Formation of monofunctional linear silylene groups by condensation between terminal silyl sites $-SiCl_2Me$:

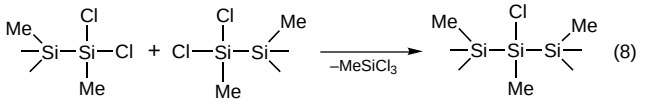

(8)

(2) Condensation of silyl $-SiCl_2Me$ and silylene groups >SiClMe:

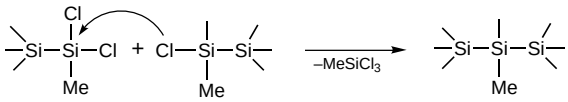

(9)

8

Si−C bonds are not cleaved at these reaction temperatures. The similar polarization inversion behaviors observed for the tertiary and linear units compared to the terminal units, in both ^{29}Si and ^{13}C experiments, suggest that the linear units are predominantly bonded to tertiary units. In addition the C.D. value of 2.27 implies cyclization steps favored leading to a polycyclic polysilane network as illustrated in Figure 18.

Such cyclic structures could explain the presence of two ^{29}Si resonance peaks assigned to linear units: the peak B_1 at 14 ppm could be related to linear units in oligosilane-type structures, while the peak B_2 at 24 ppm could be tentatively assigned to linear units in ring systems. A chemical shift of 12.8 ppm has been reported for the linear unit in the isoheptasilane $[(MeCl_2Si)_2SiMe]_2SiClMe$ **7**.[26]

IV.2. Polysilane-to-Poly(carbosilane) Transformation (180−450 °C). The increase of reaction temperature additionally activates Si−C as well as C−H bonds of the polysilane skeleton. The Si backbone atom environment is considerably changed by an increase of the number of bonded C atoms caused by the formation of carbosilane units (Si−CH_2−Si) by either Si−Si or Si−

Table 6. Estimations from the ^{29}Si and ^{13}C NMR Results of the Number of Si−Cl, Si−C, and Si−Si Bonds (n(Si−Cl) Found from Chemical Analysis Added for Comparison)

	n(Si−Cl)			n(Si−C)		n(Si−Si)	
T (°C)	chem analysis	^{29}Si NMR	^{13}C NMR	^{29}Si NMR	^{13}C NMR	^{29}Si NMR	^{13}C NMR
180	0.58	0.75	0.73	1.00	1.00	2.25	2.27
200	0.54	0.68	0.67	1.00	1.00	2.33	2.33
220	0.49	0.58		1.00	1.00	2.42	
300	0.29	0.49	0.48	1.00	1.00	2.51	2.52
300		0.35		1.07		2.58	
325	0.25	0.30		1.09		2.61	
355	0.19	0.28		1.05		2.67	
380	0.13	0.19		1.16		2.65	
400	0.08	0.17		1.38		2.45	
450	0.09	0.15		1.59		2.26	

Cl bond replacement. Indeed these groups were clearly identified in both ^{13}C and ^{29}Si NMR investigations. The carbosilane formation comes with evolution of pyrolysis gases, such as HCl, H_2, and CH_4 (Figure 17). The occurrence of several gaseous pyrolysis products as well as well defined gas-evolution steps suggests the overlap of different formation mechanisms. The modification of the polysilane backbone can be visualized synthetically through the number of Si−Cl, Si−Si, and Si−C bonds per Si atom that can be calculated from the ^{29}Si NMR results according to the following equations:

$$n(\text{Si−Cl}) = \%(B_1) + \%(B_2) + 2 \times \%(C) + \%(J) \quad (10)$$

$$n(\text{Si−C}) = \%(A_1) + \%(A_2) + \%(B_1) + \%(B_2) + \%(C) + \%(D) + 2 \times \%(F) + 3 \times \%(G) + 4 \times \%(H) + 2 \times \%(J) \quad (11)$$

$$n(\text{Si−Si}) = 3 \times \%(A_1) + 3 \times \%(A_2) + 2 \times \%(B_1) + 2 \times \%(B_2) + \%(C) + \%(D) + 4 \times \%(E) + 2 \times \%(F) + \%(G) + \%(J) \quad (12)$$

%(X) represents the relative intensity of peak X.

For comparison, similar calculations have been performed with the ^{13}C NMR results up to 300 °C. Above this temperature, the nature of the carbosilane sites is not known precisely enough to allow such estimation.

$$n(\text{Si−Cl}) = \%(b) + 2 \times \%(c) \quad (13)$$

$$n(\text{Si−C}) = \%(a) + \%(b) + \%(c) + \%(d) \quad (14)$$

$$n(\text{Si−Si}) = 3 \times \%(a) + 2 \times \%(b) + \%(c) + 3\%(d) \quad (15)$$

The results are reported in Table 6: they are in quite good agreement. The n(Si−Cl) values extracted from NMR are higher than that derived from chemical analysis, but they show a similar trend in the evolution versus reaction temperature. It should be pointed out that reliable chemical analysis results on such highly reactive and cross-linked polymers are difficult to obtain. The variation of n(Si−Cl), n(Si−C), and n(Si−Si) is represented in Figure 19.

The 180−450 °C reaction temperature range can be divided into two main stages:

(i) From 180 to 350 °C: building up of a polycyclic polysilane network according to eqs 8 and 9. A new peak (peak d) due to tertiary units appears above 180 °C in the ^{13}C NMR spectra (Figure 9) and continuously increases in intensity. It is mainly responsible for the increase in cross-linking degree in this temperature range and thus could be directly related to the formation of polycyclic network.

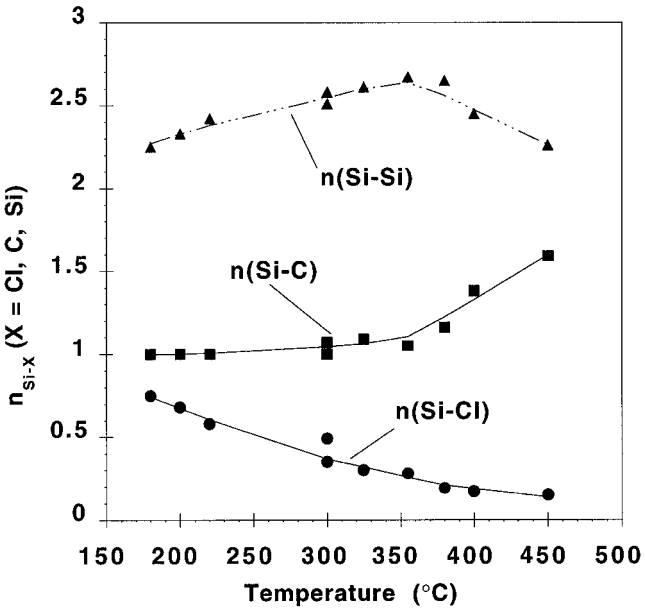

Figure 19. Evolution versus reaction temperature of the number of Si−Cl, Si−C, and Si−Si bonds per Si atom, extracted from the ^{29}Si NMR results.

(ii) Above 350 °C: degradation of the polysilane skeleton due to an enhanced cleavage of Si−Si and formation of Si−C bonds. The carbosilane formation under destruction of Si−Si bonds called "Kumada rearrangement" (eq 6) is well known to occur in methyl-containing polysilanes above 350 °C (eq 6).[39,41]

Figure 19 shows clearly a decrease of the number of Si−Si bonds and a strong increase of the number of Si−C bonds, while the Cl content remains quite constant in this temperature range. Both ^{13}C and ^{29}Si NMR results have shown unambiguously the formation of carbosilane units. Analysis of the ^{13}C IRCP data demonstrated the presence of CH_2 groups for $T > 380$ °C. The ^{29}Si NMR spectra have shown clearly several kinds of carbosilane units which were assigned to the various $(-CH_2)_xMe_ySi(Si)_{4-x-y}$ sites ($y < x \leq 4$; $y \leq 1$).

However, if carbosilane formation through a "Kumada rearrangement" occurs, the simultaneous formation of Si−H bonds is expected. But in the present case no Si sites with Si−H bonds were identified through the IRCP experiments, which should be very sensitive to such sites according to the results presented previously on the Yajima polycarbosilane. One possible explanation is the immediate consumption of as-formed Si−H groups in subsequent reactions like dehydrocoupling (16) or dehydrohalogenation (17) reactions:

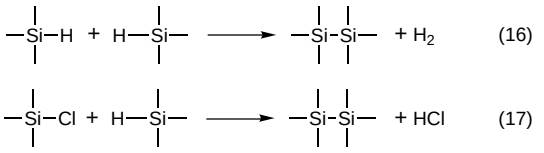

Indeed, in this temperature range, HCl, and also hydrogen, are detected in the TG/MS experiment. Methane is also formed and can result from reaction 18, for example:

(41) Sakurai, H.; Koh, R.; Hosomi, A.; Kumada, M. *Bull. Chem. Soc. Jpn.* **1966**, *39*, 2050.

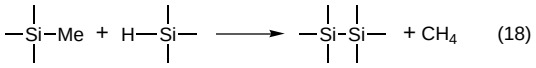

(18)

An interesting feature is the evolution of HCl in the lower temperature range 200−350 °C, where a cleavage of Si−C bonds according to eq 6 is very unlikely. This is confirmed by the absence of pyrolysis gases such as CH_4 or H_2. Furthermore, the NMR results show clearly the enhanced growth of the polysilane network. For these reasons we suggest that in this temperature range, HCl should be the condensation product of Si−Cl and H−C groups (Si−CH_3), leading to the formation of carbosilane units while Si−Si bonds are preserved:

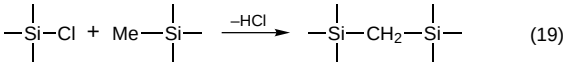

(19)

Indeed in this temperature range, carbosilane units were identified in the ^{29}Si NMR experiments, through the presence of minor peaks D and F, whose intensity never exceeds 10%, suggesting that these reactions do not occur extensively. This low carbosilane amount could explain why no peak due to CH_2 groups was detected in the ^{13}C NMR spectra. According to eq 19, formation of (−CH_2)*Si*(Si)$_3$ units (peak D) could result from condensation of a tertiary unit either with a linear unit (eq 20) or with a terminal unit (eq 21), leading respectively to the formation of (−CH_2)Me*Si*< units (peak F) or (−CH_2)MeClSi− units (peak J):

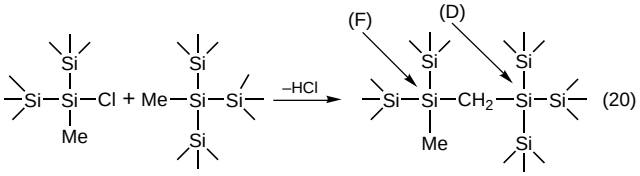

(20)

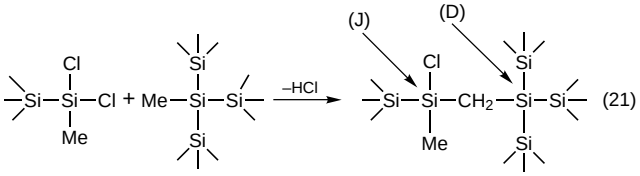

(21)

The absence of peak F below 300 °C strongly suggests that reaction 21 occurs in the 200−300 °C range and being responsible for the presence of peak D. Peak J may be present but will overlap with peak B_2 and thus is hard to identify as already mentioned previously. Above 300 °C, reaction (20) can account for the presence of peak F.

It should be emphasized as well that above 300 °C, formation of quaternary Si units, Si(Si$_4$), occurs simultaneously with that of carbosilane units (Figure 16) and reaches 18% at 450 °C. Their presence might be related to the formation of C-rich carbosilane units, such as Si-(CH_2)$_4$, which correspond to a C/Si molar ratio equal to 2. But since the present samples have a total C/Si ratio equal to 1, the local availability of carbon to form Si−C bonds is limited. This might explain the formation of Si(Si)$_4$ units.

V. Conclusions

The polysilane-to-poly(carbosilane) transformation of poly(methylchlorosilanes) (MCPS) has been investigated by ^{29}Si and ^{13}C MAS NMR, using the inversion recovery cross-polarization (IRCP) sequence. Thus far this sequence has never been used to characterize polysilanes or poly(carbosilanes) and was shown in the present study to bring very interesting structural information. Simulations of the series of IRCP spectra allowed a precise identification of the various resonance peaks, even in case of extensive peak overlap. Assignments of the various ^{29}Si and ^{13}C sites could thus be given after analysis of the inversion polarization behavior of the corresponding peaks. The formation of $^{13}CH_2$ groups was unambiguously identified from the ^{13}C IRCP measurements while ^{29}Si IRCP experiments proved to be quite efficient to distinguish between silane sites and C-rich carbosilane sites. Analysis of the CP experiments leads to a complete quantification of the various sites.

The CP and IRCP NMR results combined with results of TG/MS experiments showed that the formation of carbosilane sites (Si−CH_2−Si) starts already in the low-temperature range above 180 °C with evolution of HCl. HCl is obviously the condensation product of Si−Cl and H−C groups leading to the formation of carbosilane units without Si−Si bond cleavage (Si−Cl bond replacement). At higher temperatures (>380 °C) it is suggested that a "Kumada-rearrangement" occurs, i.e., the replacement of Si−Si by Si−C bonds, causing the transformation of the polycyclic polysilane into a poly(carbosilane) network.

The present study should be considered as a striking example to illustrate how the combined use of CP and IRCP techniques can allow a precise identification and quantification of different ^{13}C and ^{29}Si sites in preceramic polymers. Such investigation could be of high importance to characterize the first steps of the polymer-to-ceramic transformation, in the field of polysilanes, by also polysilazanes or even polyborazines, for which IRCP technique could be used to characterize ^{15}N environments.

Acknowledgment. The authors would like to greatly thank the Deutsche Forschungsgemeinschaft and NATO for financial support.

Supporting Information Available: Figures giving examples of simulations of ^{13}C and ^{29}Si IRCP MAS NMR spectra of the 180 °C MCPS and tables reporting the results of the analysis of the ^{29}Si and ^{13}C CP and IRCP MAS NMR spectra of MCPS samples reacted at various reaction temperatures (6 pages). Ordering information is given on any current masthead page.

CM960002B